DOI: 10.2352/ISSN.2470-1173.2016.15.IPAS-192

2-D Left-Side Quaternion Discrete Fourier Transform: Fast Algorithm

Artyom M. Grigoryan and Sos S. Agaian;

Department of Electrical and Computer Engineering, The University of Texas at San Antonio; One UTSA Circle, San Antonio, USA TX 78249

e-mail: amgrigoryan@utsa.edu, sos.agaian@utsa.edu

Abstract

Two-dimension discrete Fourier transform (2-D DFT) is a fundamental tool in grays-scale image processing. In color imaging, this transform is used to process separately color channels and such processing does not consider interactions between the color channels. The concept of the quaternion discrete Fourier transform (QDFT) became a very popular topic in color imaging. The color image from one of the color model, for instance the RGB model, can be transformed into the quaternion algebra and be represented as one quaternion image which allows to process simultaneously of all color components of the image. In this work, we describe the algorithm for the 2-D left-side QDFT which is based on the concept of the tensor representation when the color or quaternion image is described by a set of 1-D quaternion signals and the 1-D left-side QDFTs over these signals determine values of the 2-D left-side QDFT at corresponding subset of frequency-points. The efficiency of the tensor algorithm for calculating the fast left-side 2-D QDFT is described and compared with the existent methods.

INTRODUCTION

The discrete Fourier transform (DFT) with its fast algorithm (FFT) plays a fundamental role in several application, such as signal processing, image enhancement, image de-nosing, audio/image/video compression, image encryption, watermarking, compressive sensing, and communication systems [1]-[7]. The traditional Fourier transform is used effectively for gray-scale images. For color images, the processing in the frequency domain is reduced to processing separately color channels which do not consider interactions between the color channels. The three color channels of an image may be represented as a vector field of quaternion numbers [8], allowing for simultaneous analysis of all color data [14]-[20]. In the quaternion algebra, there are different definitions of the 2-D quaternion discrete Fourier transform. They include the two-sided 2-D QDFT, the left-side and right-side 2-D QDFTs [10]-[16],[59]. The fast QDFT algorithms are based on representation of the QDFT by combinations of a few classical 1-D DFT transforms. This allows QDFT for fast numerical implementation with the standard FFT softwares [60].

In this paper, we introduce the concept of the tensor representation of the color image in the quaternion algebra [8] which allows for effective calculation of the 2-D left-side 2-D QDFT [9, 22]. The proposed tensor algorithm is compared with the existent methods of calculation of the 2-D left-side QDFT. The complexity of the described algorithms of the left-side 1-D and 2-D QDFTs are given. The concept of the tensor representation of 2-D and multidimensional images, fast algorithms, and the theory of splitting the discrete Fourier transforms by 1-D DFTs of the splitting-signals that uniquely represent the image was first introduced and developed by Grigoryan [24]-[30] and used not only for fast calculation of the 1-D, 2-D, and 3-D DFTs, cosine, Hadamard, and Hartley transforms [32]-[38], and for image reconstruction from projections in computed tomography [40]-[51], image enhancement [21, 23],[39],[54]-[56], and filtration [4, 57]. The main results of this theory and algorithms of calculations of 2-D and 3-D DFTs of different orders as mentioned in [49] were published by other authors by different names [52, 53], including the discrete Radon transform [Gertner, 1988], the fast multidimensional Radon transform [Labunets, 1999], the finite Radon transform [Matúš and J. Flusser, 1993], the exact discrete Radon transform [Guèdon, Barba, and Burger 1995] the mojette transform [Guèdon and Normand, 2005], the discrete periodic Radon transform [Hsung, Lun, and Siu, 1996], the orthogonal discrete periodic Radon transform [Lun, Hsung, and Shen, 2003], [A. Kingston, 2006], and the generalized finite Radon transform [A. Kingston and I. Svalbe, 2007]. All these names of transforms relate to the original tensor and modified tensor representation which Grigoryan called the paired representation [25, 29, 30, 31, 4].

QUATERNION and COLOR IMAGES

The generalization of complex numbers and arithmetic is known as hyper complex numbers, and we consider the quaternion arithmetic, where attend was made to add more imaginary numbers similar to the imaginary unit i for complex numbers. To get the arithmetic with the division the number of such units as known should be 3 or 7, and the number 3 relates to quaternions.

The complex numbers $z = x + iy$ represent the points (x, y) in the complex space C. Figure shows such a plane in part a. The adding one new imaginary line to the complex plane does not result in a full arithmetic with multiplication and division. Instead,

©2016 Society for Imaging Science and Technology
DOI: 10.2352/ISSN.2470-1173.2016.15.IPAS-192

we may think to "add" similar complex planes, formally writing this operation as $C + jC$ as shown in part b.

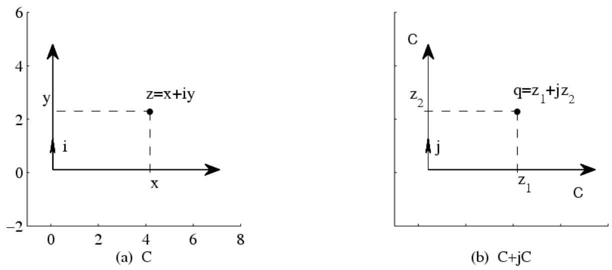

FIGURE 1: (a) The complex plane C and (b) the abstract combination of two complex spaces.

For that, we can imagine two complex planes; one complex plane C with numbers $z_1 = x_1 + iy_1$ and another complex plane C with numbers $z_2 = x_2 + iy_2$. If we assume another imaginary unit, j, then the following numbers can be considered:

$$q = z_1 + jz_2 = (x_1 + iy_1) + j(x_2 + iy_2). \tag{1}$$

We can denote such a double complex space C^2 and call such a representation of numbers q to be *the* $(2,2)$*-representation.*

Thus, the complex numbers z_1 and z_2 in this construction play the same role as the real numbers x and y in the complex numbers $x + iy$. These new numbers q can be written as

$$q = x_1 + iy_1 + jx_2 + (ji)y_2$$

where the number (ij) should represent another number, or may be an imaginary number unit, which will be denoted by k or $-k$, i.e., $k = ji$ or $-k = ji$. These numbers as elements of four (or "quaternion" in Latin) are called *quaternions* and first have been described by an English mathematician Hamilton [8].

The quaternion can be considered as a four-dimensional generation of a complex number with one real part and three-component imaginary part. The imaginary dimensions are represented as i, j, and k. In practice, the i, j, and k are orthogonal to each other and to the real numbers. Any quaternion may be represented in a hyper-complex form as

$$Q = a + bi + cj + dk = a + (bi + cj + dk),$$

where a, b, c, and d are real numbers and i, j, and k are three imaginary units with multiplication laws:

$$\begin{array}{ll} ij = -ji = k, & jk = -kj = i, \\ ki = -ik = -j, & i^2 = j^2 = k^2 = ijk = -1. \end{array}$$

The number a is considered to be the real part of Q and $(bi + cj + dk)$ is the "imaginary" part of Q. The quaternion conjugate $\bar{Q} = a - (bi + cj + dk)$. The property of commutativity does not hold in quaternion algebra, i.e., $Q_1Q_2 \neq Q_2Q_1$ for many quaternions Q_1 and Q_2.

A quaternion number has four components, a real part and three imaginary parts, which naturally coincides with the three components, R(ed), G(reen), and B(lue) of a color pixel for 2-D images. Therefore, a discrete color image $f_{n,m}$ in the RGB color space can be transformed into imaginary part of quaternion numbers form by encoding the red, green, and blue components of the RGB value as a pure quaternion (with zero real part):

$$f_{n,m} = 0 + i(r_{n,m} + jg_{n,m} + kb_{n,m}k).$$

In quaternion imaging, each color triple is treated as a whole unit [20], and it thus is expected, that by using quaternion operations, a higher color information accuracy can be achieved.

Left-side 1-D QDFT

As the generalization of the traditional Fourier transform, the quaternion Fourier transform was first defined by Ell to process quaternion signals [9]. In recent years, many works related to the quaternion discrete Fourier transform (QDFT) and its application in color image processing have been published [10, 11] and [17]. The computation the 2-D QDFT of a color image as a one unit, not by color components separately, have found many interesting application in image enhancement [12, 21, 54, 43].

Let $f_n = (a_n, b_n, c_n, d_n) = a_n + ib_n + jc_n + kd_n$ be the quaternion signal of length N. The left-side 1-D quaternion DFT (ls-QDFT) is defined as

$$F_p = Q_1(p) + iQ_i(p) + jQ_j(p) + kQ_k(p) = \sum_{n=0}^{N-1} W_\mu^{np} f_n,$$

where $p = 0 : (N-1)$ and μ is a unit pure quaternion $\mu = im_1 + jm_2 + km_3$, $\mu^2 = -1$. The kernel of this transform is

$$W_\mu = W_{N;\mu} = \exp(-\mu 2\pi/N) = \cos(2\pi/N) - \mu \sin(2\pi/N).$$

Given an angle ϕ, the multiplication of two quaternion numbers $\exp(-\mu\phi)$ and $f = a + ib + jc + kd$ can be written as

$$\begin{aligned} \exp(-\mu\phi) \cdot f = & \left(\cos(\phi) - [im_1 + jm_2 + km_3]\sin(\phi)\right) \\ & \cdot (a + ib + jc + kd) \\ = & \ a\cos(\phi) + (bm_1 + cm_2 + dm_3)\sin(\phi) \\ & + i\left[b\cos(\phi) - (am_1 + dm_2 - cm_3)\sin(\phi)\right] \\ & + j\left[c\cos(\phi) - (-dm_1 + am_2 + bm_3)\sin(\phi)\right] \\ & + k\left[d\cos(\phi) - (cm_1 - bm_2 + am_3)\sin(\phi)\right]. \end{aligned} \tag{2}$$

This equation is simple to implement in calculation of the 1-D left-side QDFT.

Let φ_{np} be the angle $(2\pi/N)np$. For a real signal x_n of length N, we consider the traditional N-point DFT of a signal x_n,

$$X_p = \sum_{n=0}^{N-1} W^{np} x_n, \quad p = 0 : (N-1),$$

where the kernel $W = W_N = W_{N;i} = \exp(-i2\pi/N) = \cos(2\pi/N) - i\sin(2\pi/N)$. We now define the following cosine and sine transforms being the real and imaginary parts of this 1-D DFT:

$$\begin{aligned} C_x(p) &= \mathrm{Real}(X_p) = \sum_{n=0}^{N-1} x_n \cos(\varphi_{np}), \\ S_x(p) &= -\mathrm{Imag}(X_p) = \sum_{n=0}^{N-1} x_n \sin(\varphi_{np}), \end{aligned} \tag{3}$$

where $p = 0 : (N-1)$.

We denote the vector of coefficients $(C_x(0), C_x(1), C_x(2), \ldots, C_x(N-1))$ by $C(x)$, and vector $(S_x(0), S_x(1), S_x(2), \ldots,$

©2016 Society for Imaging Science and Technology
DOI: 10.2352/ISSN.2470-1173.2016.15.IPAS-192

$S_x(N-1))$ by $S(x)$. The four vectors composed by the coefficients $Q_1(p)$, $Q_i(p)$, $Q_j(p)$, and $Q_k(p)$ are denoted by Q_1, Q_i, Q_j, and Q_k, respectively. As follows from (2), the 1-D left-side QDFT can be written as

$$\begin{aligned}
&Q_1 + iQ_i + jQ_j + kQ_k = \\
&= C(a) + m_1 S(b) + m_2 S(c) + m_3 S(d) \\
&= i\left[C(b) - m_1 S(a) - m_2 S(d) + m_3 S(c)\right] \\
&= j\left[C(c) + m_1 S(d) - m_2 S(a) - m_3 S(b)\right] \\
&= k\left[C(d) - m_1 S(c) + m_2 S(b) - m_3 S(a)\right].
\end{aligned} \tag{4}$$

This equation can also be writen as

$$\begin{aligned}
&Q_1 + iQ_i + jQ_j + kQ_k = \\
&= C(a) + m_1 S(b) + m_2 S(c) + m_3 S(d) \\
&= i[-m_1 S(a) + C(b) + m_3 S(c) - m_2 S(d)] \\
&= j[-m_2 S(a) - m_3 S(b) + C(c) + m_1 S(d)] \\
&= k[-m_3 S(a) + m_2 S(b) - m_1 S(c) + C(d)].
\end{aligned} \tag{5}$$

Therefore, if we denote the N-point 1-D DFTs of the parts a_n, b_n, c_n, and d_n of the quaternion signal f_n by A_p, B_p, C_p, and D_p, respectively, we obtain the following algorithm of calculation of the 1-D left-side QDFT:

$$F_p = Q_1(p) + iQ_i(p) + jQ_j(p) + kQ_k(p),$$

$$\begin{aligned}
Q_1(p) &= \mathrm{Real}(A_p) + m_1 \mathrm{Imag}(B_p) \\
&\quad + m_2 \mathrm{Imag}(C_p) + m_3 \mathrm{Imag}(D_p) \\
Q_i(p) &= -m_1 \mathrm{Imag}(A_p) + \mathrm{Real}(B_p) \\
&\quad + m_3 \mathrm{Imag}(C_p) - m_2 \mathrm{Imag}(D_p) \\
Q_j(p) &= -m_2 \mathrm{Imag}(A_p) - m_3 \mathrm{Imag}(B_p) \\
&\quad + \mathrm{Real}(C_p) + m_1 \mathrm{Imag}(D_p) \\
Q_k(p) &= -m_3 \mathrm{Imag}(A_p) + m_2 \mathrm{Imag}(B_p) \\
&\quad - m_1 \mathrm{Imag}(C_p) + \mathrm{Real}(D_p)
\end{aligned} \tag{6}$$

where $p = 0 : (N-1)$.

One can note that no more than $12N$ operations of real multiplications plus 4 times $m_{DFT}(N)$ are used for $m_{QFT}(N)$. Thus, the number of operations of multiplication and addition equal $m_{QFT}(N) = 4m_{FT}(N) + 12N$ and $a_{QFT}(N) = 4a_{FT}(N) + 12N$.

We consider the case when $N = 2^r$, $r > 2$. The paired transform algorithm for the N-point DFT uses the real multiplications and additions in numbers [4, 29, 23, 30]:

$$\begin{aligned}
&4 \times \mu_{FT}(N) = 4 \times [2^{r-1}(r-3) + 2] \\
&2 \times \alpha_{FT}(N) = 2 \times [(2^r 6 - r^2 - 3r - 6) + \mu_{FT}(N)].
\end{aligned} \tag{7}$$

It is assumed that the complex multiplication is performed with two additions and four multiplications. Since the calculation of two N-point DFTs over the real signals can be reduced to one N-point DFT of a complex signal, we assume that $2m_{FT}(N) = 4 \times \mu_{FT}(N)$ and $2a_{FT}(N) = 2 \times \alpha_{FT}(N)$. The number of operations for calculating the N-point DFT of the real signal is twice less than the number of operations for the transform of complex signal. Two 1-D DFTs with real inputs can be calculated by one DFT with complex input [23]. Therefore, the number of operations when calculating the 1-D left-side QDFT can be estimated as

$$\begin{aligned}
m_{QFT}(N) &= 8\mu_{FT}(N) + 12N = 4Nr + 16, \\
a_{QFT}(N) &= 4\alpha_{FT}(N) + 12N = 2N(r+15) \\
&\quad -4(r^2 + 3r + 4).
\end{aligned} \tag{8}$$

We should note that the same numbers of multiplication and addition are used for the 1-D right-side QDFT [58].

In the special case when $\mu = (i + j + k)/\sqrt{3}$, equation (8) can be written as

$$F_p = Q_1(p) + iQ_i(p) + jQ_j(p) + kQ_k(p),$$

$$\begin{aligned}
Q_1(p) &= \mathrm{Real}(A_p) + [\mathrm{Imag}(B_p) + \mathrm{Imag}(C_p) \\
&\quad + \mathrm{Imag}(D_p)]/\sqrt{3}, \\
Q_i(p) &= \mathrm{Real}(B_p) - [\mathrm{Imag}(A_p) - \mathrm{Imag}(C_p) \\
&\quad + \mathrm{Imag}(D_p)]/\sqrt{3}, \\
Q_j(p) &= \mathrm{Real}(C_p) - [\mathrm{Imag}(A_p) + \mathrm{Imag}(B_p) \\
&\quad - \mathrm{Imag}(D_p)]/\sqrt{3}, \\
Q_k(p) &= \mathrm{Real}(D_p) - [\mathrm{Imag}(A_p) - \mathrm{Imag}(B_p) \\
&\quad + \mathrm{Imag}(C_p)]/\sqrt{3},
\end{aligned} \tag{9}$$

where $p = 0 : (N-1)$. The number of operations of multiplication and addition equal $m_{QFT}(N) = 4m_{FT}(N) + 4N$, or $8N$ operations of real multiplication less than in (8).

The Left-Side 2-D QDFT

The quaternion multiplication is not commutative and the definition of the 2-D DQFT is not unique [11]-[13],[60]. Different DQFT can be used in image processing, including the left-side, right-side, and two-side DQFTs. In this section, we consider the left-side 2-D DQFT. The color image $f_{n,m}$ is considered to be of size $N \times M$ which is transformed form RGB color model to the quaternion subspace, namely the subspace of pure quaternions.

Let N_0 be the g.c.d.(N,M) and $N = N_0 N_1$, $M = N_0 M_1$, and $K = M_1 N = N_1 M$, where integers $N_1, M_1 \geq 1$. The left-side 2-D QDFT of the complex-in-quaternion image $f_{n,m}$ is defined as

$$F_{p,s} = \sum_{n=0}^{N-1} W_{N;\mu}^{np} \left[\sum_{m=0}^{M-1} W_{M;\mu}^{ms} f_{n,m} \right],$$

where $p = 0 : (N-1)$ and $s = 0 : (M-1)$. This transform can also be written as [13]:

$$F_{p,s} = \sum_{n=0}^{N-1} \sum_{m=0}^{M-1} W_{K;\mu}^{M_1 np + N_1 ms} f_{n,m},$$

where $p = 0 : (N-1)$ and $s = 0 : (M-1)$. Here, for a given quaternion unit number μ, the basis exponential function is

$$W_{K;\mu} = \exp(-2\pi\mu/K) = \cos(2\pi/K) - \mu \sin(2\pi/K).$$

This is the left-side 2-D QDFT.

The inverse left-side 2-D QDFT is calculated by

$$f_{n,m} = \frac{1}{NM} \sum_{p=0}^{N-1} \sum_{s=0}^{M-1} W_{K;\mu}^{-(M_1 np + N_1 ms)} F_{p,s},$$

where $p = 0 : (N-1)$ and $s = 0 : (M-1)$.

With the direct calculation, the separable 2-D left-side QDFT requires N M-point 1-D left-side QDFTs and M N-point 1-D left-side QDFTs. The 1-D left-side QDFT requires two 1-D DFTs. Therefore, the row-column method uses $2N$ M-point 1-D DFTs and $2M$ N-point 1-D DFTs.

As an example, Figure 2 shows the color image of size 1223×1223; the number 1223 is prime.

©2016 Society for Imaging Science and Technology
DOI: 10.2352/ISSN.2470-1173.2016.15.IPAS-192

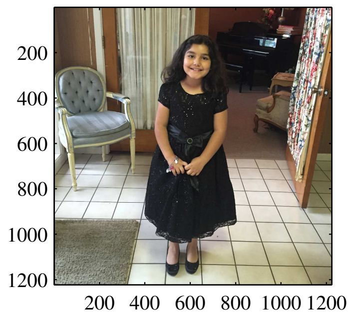

FIGURE 2: The color '‘girl Anoush” image.

Tensor Representation and the left-side 2-D QDFT

For the simplicity of calculation, we consider the $N=M=K$ case, i.e., when the left-side 2-D $N \times N$-point QDFT of the color-in-quaternion image $f_{n,m}$ is

$$F_{p,s} = \sum_{n=0}^{N-1}\sum_{m=0}^{N-1} W_\mu^{np+ms} f_{n,m}, \quad p,s = 0:(N-1). \tag{10}$$

It is important to note that the kernel of this transform is periodic,

$$\begin{aligned} W_\mu^{t+N} &= \cos(2\pi(t+N)/N) - \mu \sin(2\pi(t+N)/N) \\ &= \cos(2\pi t/N) - \mu \sin(2\pi t/N) = W_\mu^t, \end{aligned}$$

when $t = 0:(N-1)$. Therefore, for the left-side 2-D QDFT, we can apply the concept of the tensor representation [4, 43] and reduce the calculation and processing of this transform to processing of 1-D signals, which we call the color splitting-signals, or the quaternion splitting-signals.

In the absolute scale, the left-side 2-D QDFT of the color image is shown in Figure 3. This transform is shifted to the center.

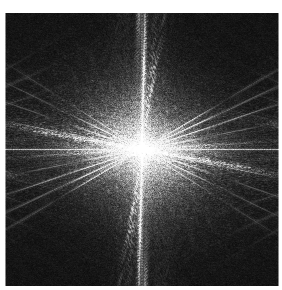

FIGURE 3: (a) The left-side 2-D QDFT of the 2-D color-in-quaternion ‘girl Anoush” image in the absolute scale and shifted cyclicly to the center.

We consider the color image

$$f_{n,m} = (r_{n,m} i + g_{n,m} j + b_{n,m} k)$$

with zero real part in the quaternion algebra. The tensor representation of the discrete image is the 2-D frequency and 1-D time representation, when the image is described by a set of 1-D splitting-signals of length N each,

$$\chi : \{f_{n,m}\} \to \left\{ f_{T_{p,s}} = \{f_{p,s,t}; t = 0:(N-1)\} \right\}_{(p,s)\in J_{N,N}}.$$

This transform, as mentioned in Introduction, in many publications is also named as discrete Radon transform.

Given (p,s), the components of the splitting-signal $f_{T_{p,s}}$ are the following sums (or ray-sums) of the image $f_{n,m}$ along the parallel lines on the Cartesian lattice

$$X = X_{N,N} = \{(n,m); n,m = 0,1,...,(N-1)\},$$

i.e.,

$$f_{p,s,t} = \sum_{(n,m)\in X} \{f_{n,m}; np+ms = t \bmod N\}.$$

This quaternion splitting-signal $f_{T_{p,s}} = \{f_{p,s,t}; t = 0:(N-1)\}$ is calculated as

$$\begin{aligned} f_{p,s,t} &= i(r_{p,s,t}) + j(g_{p,s,t}) + k(b_{p,s,t}) \\ &= \sum_{(n,m)\in V_{p,s,t}} f_{n,m} = i\left(\sum_{(n,m)\in V_{p,s,t}} r_{n,m}\right) \\ &\quad + j\left(\sum_{(n,m)\in V_{p,s,t}} g_{n,m}\right) + k\left(\sum_{(n,m)\in V_{p,s,t}} b_{n,m}\right). \end{aligned} \tag{11}$$

Here, for a given generator (p,s) from the set $J_{N,N}$, we define the following N subsets in the Cartesian lattice:

$$V_{p,s,t} = \{(n,m) \in X; np+ms = t \bmod N\}, \quad t = 0:(N-1).$$

The imaginary components of the splitting-signals are the splitting-signals of the red, green, and blue channels of the color image.

The frequency-point (p,s) is called the generator of the splitting-signal. The components $f_{p,s,t}$ are periodic by t, i.e., $f_{p,s,t+N} = f_{p,s,t}$. We denote this splitting-signal by the set

$$T_{p,s} = \left\{(kp \bmod N, ks \bmod N); k = 0:(N-1)\right\},$$

since the signal carries the information about the 2-D DFT at N frequency-points of this set [30, 4],

$$F_{kp \bmod N, ks \bmod N} = \sum_{t=0}^{N-1} f_{p,s,t} W_\mu^{kt}, \quad k = 0:(N-1). \tag{12}$$

Indeed, the union of the family of disjoint subsets $V_{p,s,t}$, $t = 0:(N-1)$, is the Cartesian grid and, therefore, the following calculations hold:

$$\begin{aligned} &\sum_{t=0}^{N-1} f_{p,s,t} W_\mu^{kt} = \\ &= \sum_{t=0}^{N-1}\left[\sum_{np+ms=t \bmod N} (r_{n,m})i + (g_{n,m})j + (b_{n,m})k\right] W_\mu^{kt} \\ &= \sum_{t=0}^{N-1}\left(\sum_{np+ms=t \bmod N} (r_{n,m})i + (g_{n,m})j + (b_{n,m})k\right) W_\mu^{k(np+ms)} \\ &= \sum_{n=0}^{N-1}\sum_{m=0}^{N-1}\Big((r_{n,m})i + (g_{n,m})j + (b_{n,m})k\Big) W_\mu^{n(kp)+m(ks)}. \\ &= \sum_{n=0}^{N-1}\sum_{m=0}^{N-1} f_{n,m} W_\mu^{n(kp)+m(ks)} = F_{kp \bmod N, ks \bmod N}. \end{aligned}$$

The set $J_{N,N}$ of frequency-points (p,s), or generators, of the splitting-signals is selected in a way that covers the Cartesian lattice $X_{N,N}$ with a minimum number of subsets $T_{p,s}$. For instance,

©2016 Society for Imaging Science and Technology
DOI: 10.2352/ISSN.2470-1173.2016.15.IPAS-192

when $N = 2^r$, $r > 1$, the set $J_{N,N}$ contains $3N/2$ generators and can be defined as

$$J_{N,N} = \{(1,s); s = 0 : (N-1)\} \cup \{(2p,1); p = 0 : (N/2-1)\}.$$

The tensor representation is unique, and the image can be defined through the 2-D DFT calculated by (12), or directly from the tensor transform, as shown in [4, 23, 41]. Since $3N/2$ splitting-signals compose the tensor representation, the calculation of the 2-D DFT is reduced to $3N/2$ one-dimensional N-point DFT, instead of $2N$ such transformation in the traditional row-column method.

It should be noted, that the total number of components of $3N/2$ splitting-signals equals $N^2 + N^2/2$, which exceeds the number N^2 of points in the image. On the other side, many sets $T_{p,s}$, with generators $(p,s) \in J_{N,N}$ have intersections at frequency-points. In the $N = 2^r$ case when $r > 1$, the color image is described by $3N/2$ quaternion splitting-signals and 2-D QDFT of the image is split by the $3N/2$ 1-D QDFT of these signals. The tensor transform is therefore redundant. This redundancy can be removed and the 2-D DFT can be calculated in a more effective way, by using the modification of the tensor representation, which is called the paired transform [4, 30].

The tensor representation is very effective in another case of most interest when N is a prime, since the number of required sets $T_{p,s}$ is $N+1$ and the sets intersect only at the point $(0,0)$. Now, we implement the concept of the tensor representation for the quaternion images. In this case, the number of such signals and 1-D QDFT equals $(N+1)$, because the set of generators can be taken as

$$J_{N,N} = \{(1,s); s = 0 : (N-1)\} \cup \{(0,1)\}.$$

We consider the representation of this image at frequency-point $(p,s) = (1,4)$. The components of the quaternion splitting-signals of the red, green, and blue channels, which are generated by this frequency-point $(1,4)$ are shown in Figure 4 in parts a, b, and c, respectively.

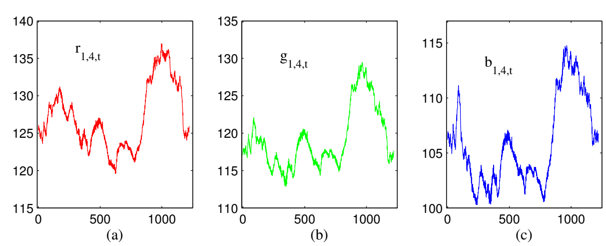

FIGURE 4: The (a) red, (b) green, and (c) blue components of the splitting-signal $f_{1,4,t}$.

In this case $N = 1223$. The set of $N+1 = 1224$ such triplet splitting-signals of length N each describe the color-in-quaternion image as well as its 2-D QDFT. The splitting-signal

$$f_{1,4,t} = (r_{1,4,t})i + (g_{1,4,t})j + (b_{1,4,t})k, \quad t = 0 : (N-1),$$

is referred to as the color splitting-signal in the quaternion space. The N-point left-side 1-D QDFT of this splitting-signal is shown in Figure 5 in the absolute scale (and with the normalized actor of $1/N^2$) only for the real part of the transform in part (a) and the i-component of the imaginary part in b.

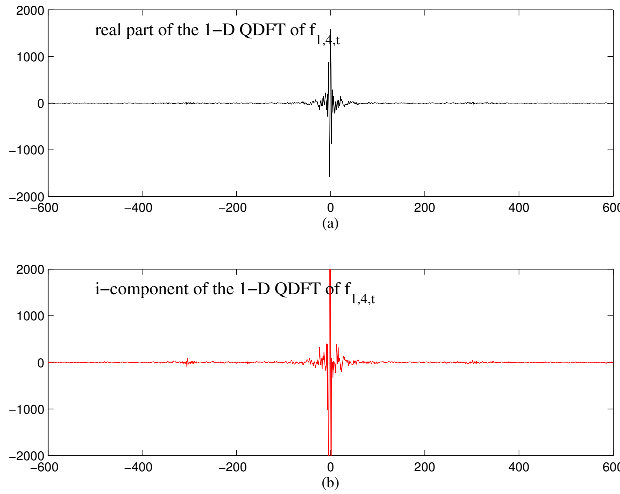

FIGURE 5: The (a) real and (b) i-component of the 1223-point left-side QDFT of the quaternion splitting-signal $f_{1,4,t}$.

In the absolute scale, the 1-D left-side QDFT of the splitting-signal is shown in Figure 6 in part a after shifting to the center. The 1-D QDFT this splitting-signal coincides with the 2-D left-side QDFT of the image at frequency-points of the set $T_{1,4}$ which are shown in part b.

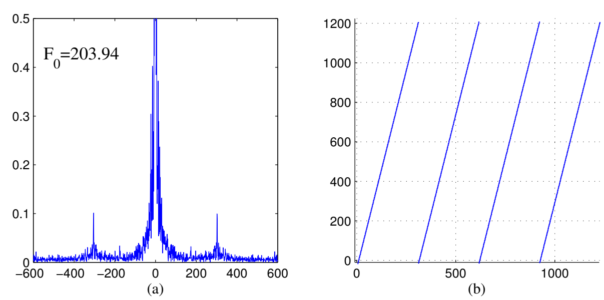

FIGURE 6: (a) The 1-D left-side QDFT the quaternion splitting-signal $f_{1,4,t}$ (in the absolute scale), and (b) the location of frequency-points of the set $T_{1,4}$ on the Cartesian grid.

Figure 7 illustrates the quaternion 2-D left-side QDFT. The real part of this quaternion transform is shown in part a in the absolute scale, and the imaginary part as three-component data is shown in the RGB color model in part a.

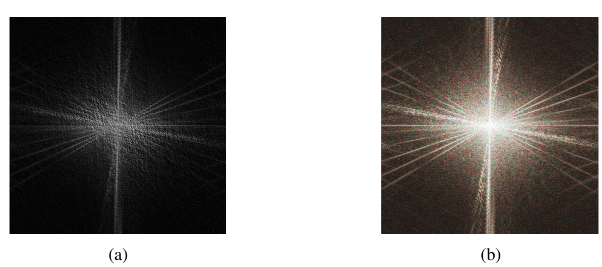

FIGURE 7: (a) The real part and (b) the imaginary part of the left-side 2-D QDFT of the 2-D color-in-quaternion 'girl Anoush"

©2016 Society for Imaging Science and Technology
DOI: 10.2352/ISSN.2470-1173.2016.15.IPAS-192

image in the absolute scale and shifted cyclicly to the center. All 1-D and 2-D quaternion left-side DFTs were calculated for the unit number $\mu = (i+2j+k)/\sqrt{6}$.

When $N = 2^r$ and integer $r > 1$, the number of N-point 1-D QDFTs required to calculate the $N \times N$-point 2-D QDFT equals $3N/2$. For $N > 2$ prime, the number of N-point 1-D QDFTs required to calculate the $N \times N$-point 2-D QDFT equals $N+1$. It should be noted, that the tensor transform is of size $N(N+1) = N^2+N > N^2$, but it is not redundant since we can represent the image by one full splitting-signal, let say $\{f_{1,0,t};\, t = 0:(N-1)\}$, and N other signals as $\{f_{p,1,t};\, t = 0:(N-2)\}$. The sum of components of splitting-signals is the same and equals the area (S) of image, i.e.,

$$\sum_{t=0}^{N-1} f_{p,1,t} = S = \sum_{n=0}^{N-1}\sum_{m=0}^{N-1} f_{n,m},$$

for all $p = 0:(N-1)$. Therefore,

$$f_{p,1,N-1} = S - \sum_{t=0}^{N-2} f_{p,1,t}.$$

Each N-point 1-D left-side QDFT can be calculated by two complex N-point 1-D DFTs. Here, we note for comparison, that the number of $N \times N$-point 2-D left-side QDFT in the traditional row-column wise algorithm requires $2N$ N-point 1-D left-side QDFTs, or $4N$ N-point complex 1-D DFTs.

The representation of the color and quaternion image by the 1-D splitting-signals allows us not only calculate the 2-D left-side QDFT, but to reconstruct the image directly from the splitting-signals,or the direction images defined by the splitting-signals. Similar to the gray-scale images [4],[39]-[42], the direction image from the signal $f_{p,s,t}$ is calculated by

$$d_{n,m} = d^{n,m;p,s} = \frac{1}{N} f_{p,s,(np+ms) \bmod N} \tag{13}$$

where $n,m = 0:(N-1)$.

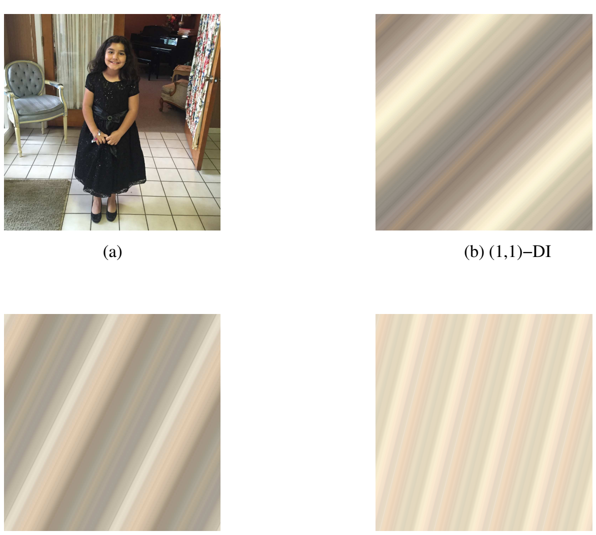

(a) (b) (1,1)–DI (c) (1,2)–DI (d) (1,4)–DI

FIGURE 8: (a) The color image and direction images generated by (p,s) equal (b) $(1,1)$, (c) (1,2), and (d) $(1,4)$.

Figure 8 shows the color image in part a, and the direction images generated by three frequency-points $(p,s) = (1,1)$, $(1,2)$ and $(1,4)$ in parts b, c, and d, respectively. These direction images were amplified by the factors of $1.5, 1.5$, and 1.85, respectively.

For this example when $N = 1223$, the color image 1223×1223 is the sum of such 1224 direction images $\{d^{n,m;p,s};\, (p,s) \in J_{1223,1223}\}$ which represents the inverse tensor transform.

In general case when N is prime, all $(N+1)$ cyclic-groups $T_{p,s}$ intersect only at points $(0,0)$. The following statements hold:

Statement 1: The quaternion image $f_{n,m}$ of size $N \times N$, where $N > 2$ is a prime, can be calculated as the sum of $(N+1)$ directional images:

$$\begin{aligned} f_{n,m} &= \sum_{(p,s)\in J_{N,N}} d_{n,m;p,s} \\ &= \frac{1}{N}\left[\sum_{p=0}^{N-1} f_{p,1,(np+m) \bmod N} + f_{1,0,n}\right], \\ & n,m = 0:(N-1). \end{aligned} \tag{14}$$

The reconstruction of the color and quaternion images by direction images has place for other cases of N. For instance for the $N = 2^r$ case, we can use the modified tensor representation which is similar to the paired representation for the 2-D gray-scale images (see for details [4, 23, 5]).

Statement 2: The quaternion discrete image of size $N \times N$, where $N = 2^r$, $r > 1$, can be composed from its $(3N-2)$ direction images as

$$\begin{aligned} f_{n,m} &= \sum_{(p,s)\in J'_{N,N}} d_{n,m;p,s} \\ &= \frac{1}{2N}\sum_{k=0}^{r-1}\frac{1}{2^k}\sum_{(p,s)\in 2^k J_{2^{r-k},2^{r-k}}} f'_{p,s,(np+ms) \bmod N} \\ &\quad + \frac{1}{N^2} f'_{0,0,0}. \end{aligned} \tag{15}$$

Here, the components $f'_{p,s,t}$ are components of the paired representation [25, 27, 30, 4] which are defined from the tensor representation by

$$f'_{p,s,t} = f_{p,s,t} - f'_{p,s,t+N/2}.$$

The last addendum in the formula represents the mean value of the image, which we denote by $E[f]$,

$$E[f] = \frac{1}{N^2} f'_{0,0,0} = \frac{1}{N^2} S.$$

Conclusion

The 2-D left-side quaternion discrete Fourier transform (QDFT) is decribed in the tensor representation in the quaternion algebra wherein the color image can be transformed from for such color models, as RGB or XYZ. The color and quaternion images are uniquely described by a set of quaternion splitting-signals which allow to calculate the 2-D left-side QDFT by a minimum number of 1-D left-side QDFTs. The proposed tensor algorithm was shown uses less number of multiplications as the existent algorithms. The tensor representation is revealing the structure of both right- and let-side 2-D QDFT, is effective, and allows for transferring the processing of color and quaternion images through 1-D splitting-signal.

References

[1] L. Rabiner, B. Gold, *Theory and application of digital signal processing,* Prentice-Hall Inc., 1975.

[2] S.S. Agaian, "Advances and problems of the fast orthogonal transforms for signal-images processing applications (Part 1)," in: *Pattern Recognition, Classification, Forecasting. Yearbook, The Russian Academy of Sciences, Nauka,* Moscow, Issue 3, pp. 146-215, 1990.

[3] Y. Zhou, W. Cao, L. Liu, S. Agaian, C.L. P. Chen, "Fast Fourier transform using matrix decomposition," *Information Sciences*, vol. 291, pp. 172-183, 2015.

[4] A.M. Grigoryan, S.S. Agaian, *Multidimensional discrete unitary transforms: Representation, partitioning and algorithms,* Marcel Dekker Inc., New York, 2003.

[5] A.M. Grigoryan, S.S. Agaian, "Split manageable efficient algorithm for Fourier and Hadamard transforms, *IEEE Trans. Signal Processing,* vol. 48, no. 1, pp. 172-183, 2000.

[6] S.S. Agaian, K. Panetta, A.M. Grigoryan, "Transform-based image enhancement algorithms," *IEEE Trans. on Image Processing,* vol. 10, no. 3, pp. 367–382, 2001.

[7] A.M. Grigoryan, S.S. Agaian, "Transform-based image enhancement algorithms with performance measure," *Advances in Imaging and Electron Physics, Academic Press,* vol. 130, pp. 165–242, 2004.

[8] W.R. Hamilton, *Elements of Quaternions,* Logmans, Green and Co., London, 1866.

[9] T.A. Ell, "Quaternion-Fourier transforms for analysis of 2-dimensional linear time-invariant partial differential systems," *In Proceedings of the 3nd IEEE Conference on Decision and Control,* vol. 1-4, pp. 1830–1841, San Antonio, Texas, USA, December 1993.

[10] E. Hitzer, "Quaternion Fourier transform on quaternion fields and generalizations," Advances in Applied Clifford Algebras, vol. 17, no. 3, pp. 497-517, May 2007.

[11] M.H. Yeh, "Relationships among various 2-D quaternion Fourier transforms," *IEEE Signal Processing Letters,* vol. 15, pp. 669-672, 2008.

[12] S.J. Sangwine, "Fourier transforms of colour images using quaternion, or hypercomplex, numbers," *Electronics Letters,* vol. 32, no. 21, pp. 1979–1980, October 1996.

[13] S.J. Sangwine, T.A. Ell, J.M. Blackledge, and M.J. Turner, "The discrete Fourier transform of a color image," *in Proc. Image Processing II Mathematical Methods, Algorithms and Applications,* pp. 430–441, 2000.

[14] T. Shaneyfelt, M. Jamshidi, and S.S. Agaian, "Hierarchical Robotic Crane System for Post Grid Array Environments," System of Systems Engineering (SoSE), 8th International Conference, pp. 83–87, 2013.

[15] A. Kolaman and O. Yadid-Pecht, "Quaternion structural similarity: A new quality index for color images," IEEE Transactions on Image Processing, 2012.

[16] Z. Yang and S.-I. Kamata, "Hypercomplex polar Fourier analysis for color image," Proceedings - International Conference on Image Processing, ICIP 2011.

[17] A. Greenblatt, C.M. Lopez, Sos S. Agaian, "Quaternion neural networks applied to prostate cancer Gleason grading, in Proceedings, Man and Cybernetics, SMC 2013. IEEE International Conference, Manchester, pp. 1144–1149, 2013.

[18] H.-Y. Gao and K.-M. Lam, "From quaternion to octonion: Feature-based image saliency detection," ICASSP, IEEE International Conference on Acoustics, Speech and Signal Processing - Proc. pp. 2808-2812, 2014.

[19] Guo, L., Dai, M., Zhu, M. "Quaternion moment and its invariants for color object classification," Information Sciences, vol. 273, pp. 132143, July 2014.

[20] A.M. Grigoryan and S.S. Agaian, "Retolling of color imaging in the quaternion algebra," *Applied Mathematics and Sciences: An International Journal (MathSJ),* vol. 1, no. 3, pp. 23-39, 2014.

[21] A.M. Grigoryan, J. Jenkinson, S.S. Agaian, "Quaternion Fourier transform based alpha-rooting method for color image measurement and enhancement," *SIGPRO-D-14-01083R1, Signal Processing,* vol. 109, pp. 269–289, April 2015, (doi:10.1016/j.sigpro.2014.11.019)

[22] S.C. Pei, J.J. Ding, and J.H. Chang, "Efficient implementation of quaternion Fourier transform, convolution and correlation by 2-D complex FFT," IEEE Trans. Signal Process., vol. 49, pp. 2783-2797, 2001.

[23] A.M. Grigoryan and M.M. Grigoryan, *Brief Notes in Advanced DSP: Fourier Analysis With MATLAB.,* CRC Press Taylor and Francis Group, 2009.

[24] A.M. Grigoryan, "An algorithm of the two-dimensional Fourier transform," *Izvestiya VUZov SSSR, Radioelectronica,* vol. 27, no. 10, pp. 52-57, USSR, Kiev 1984. (translated in http://fasttransforms.com/Art-USSR-papers/Art_IzvuzovSSSR1984.pdf)

[25] A.M. Grigoryan, "An optimal algorithm for computing the two-dimensional discrete Fourier transform," *Izvestiya VUZ SSSR, Radioelectronica*, vol. 29, no. 12, pp. 20-25, USSR, Kiev 1986. (translated in http://fasttransforms.com/Art-USSR-papers/Art_IzvuzovSSSR1986.pdf)

[26] A.M. Grigoryan, "New algorithms for calculating discrete Fourier transforms," *Journal Vichislitelnoi Matematiki i Matematicheskoi Fiziki*, vol. 26, no 9, pp. 1407-1412, AS USSR, Moscow 1986. (translated in http://fasttransforms.com/Art-USSR-papers/Art_JVMATofASUSSR1986.pdf)

[27] A.M. Grigoryan and M.M. Grigoryan, "Two-dimensional Fourier transform in the tensor presentation and new orthogonal functions," *Avtometria, AS USSR Siberian section,* no 1, pp. 21-27, Novosibirsk, 1986.

[28] A.M. Grigoryan, "An algorithm for computing the two-dimensional Fourier transform of equal orders," Proceedings of the IX All-Union Conference on Coding and Transmission of Information, Part 2, pp. 49-52, USSR, Odessa 1988. (translated in http://fasttransforms.com/Art-USSR-papers/Art_AllUnConf1988.pdf)

[29] A.M. Grigoryan, "An algorithm for computing the discrete Fourier transform with arbitrary orders," *Journal Vichislitelnoi Matematiki i Matematicheskoi Fiziki,* AS USSR, vol. 30, no. 10, pp. 1576-1581, Moscow 1991. (translated in http://fasttransforms.com/Art-USSR-papers/Art_JVMATofASUSSR1991.pdf)

[30] A.M. Grigoryan, "2-D and 1-D multi-paired transforms: Frequency-time type wavelets," *IEEE Trans. on Signal Processing,* vol. 49, no. 2, pp. 344–353, Feb. 2001.

[31] A.M. Grigoryan, "Fourier transform representation by frequency-time wavelets," *IEEE Trans. on Signal Processing,* vol. 53, no. 7, pp. 2489-2497, July 2005.

[32] A.M. Grigoryan, S.S. Agaian, "Efficient algorithm for computing the 2-D discrete Hadamard transform," *IEEE Transactions on Cir-*

©2016 Society for Imaging Science and Technology
DOI: 10.2352/ISSN.2470-1173.2016.15.IPAS-192

cuits and Systems II, vol. 47, no. 10, pp. 1098–1103, October 2000.

[33] A.M. Grigoryan, "Multidimensional Discrete Unitary Transforms," chapter 19 (69 pages), in Third Edition Transforms and Applications Handbook in The Electrical Engineering Handbook Series (Editor in Chief, Prof. Alexander Poularikas), *CRC Press, Taylor and Francis Group,* January 11, 2010.

[34] A.M. Grigoryan, Sos S. Agaian, "Shifted Fourier transform-based tensor algorithms for the 2-D DCT," *IEEE Trans. Signal Processing,* vol. 49, no. 9, pp. 2113–2126, Sep. 2001.

[35] A.M. Grigoryan and S.S. Agaian, "Three algorithms for computing the 2-D discrete Hartley transform," *ICIP 2000 Conference on Image Processing,* pp. 359–362, Sep. 2000.

[36] A.M. Grigoryan, "Paired algorithm of the 1-D discrete Hartley transform," *The International Signal Processing Conference (ISPC) and Global Signal Processing Expo (GSPx),* Dallas, March 31-April 3, 2003.

[37] S.S. Agaian, H.G. Sarukhanyan, K.O. Egiazarian, and J. Astola, Hadamard Transforms, *SPIE Press,* 2011.

[38] C. Carranza, D. Llamocca, M. Pattichis, "Fast and scalable computation of the Fourier and inverse discrete periodic Radon transform," *IEEE Trans. Signal Processing,* vol. 25, no. 1, pp. 119–133, January 2016.

[39] A.M. Grigoryan, K. Naghdali, "On a method of paired representation: Enhancement and decomposition by series direction images," *Journal of Mathematical Imaging and Vision,* vol. 34, no. 2, pp. 185–199, June 2009.

[40] A.M. Grigoryan, "Solution of the problem on image reconstruction in computed tomography," *Journal of Mathematical Imaging and Vision,* vol. 54, Issue 1, pp. 35–63, January 2016. (doi: 10.1007/s10851-015-0588-6)

[41] A.M. Grigoryan, M.M. Grigoryan, *Image processing: Tensor transform and discrete tomography with MATLAB,* CRC Press Taylor and Francis Group, 2012.

[42] A.M. Grigoryan, "Method of paired transforms for reconstruction of images from projections: Discrete model," *IEEE Transactions on Image Processing,* vol. 12, no. 9, pp. 985-994, September 2003.

[43] A. Grigoryan, S. Agaian, "Tensor form of image representation: enhancement by image-signals," in Proc. *IS&T/SPIEs Symposium on Electronic Imaging Science* & *Technology,* San Jose. CA, 22-23 January 2003.

[44] A.M. Grigoryan and N. Du, "Novel tensor transform-based method of image reconstruction from limited-angle projection data," [9020-14], *SPIE proceedings, 2014 Electronic Imaging: Computational Imaging XII,* February 2-6, San Francisco, California, 2014.

[45] F.T. Arslan, J.M. Moreno, and A.M. Grigoryan, "Paired directional transform-based methods of image enhancement," *SPIE proceedings, Visual Information Processing XV,* vol. 6246 April 18-19, 2006.

[46] F.T. Arslan, A.K. Chan, and A.M. Grigoryan, "Directional denoising of aerial images by splitting-signals," *IEEE Region 5 Technical, Professional, and Student Conference (TPS 2006),* April 6-8, San Antonio, TX.

[47] F.T. Arslan and A.M. Grigoryan, "Enhancement of medical images by the paired transform," *in Proceedings of the 14th IEEE International Conference on Image Processing,* vol. 1, pp. 537–540, San Antonio, Texas, September 16-19, 2007.

[48] A.M. Grigoryan, Nan Du, "2-D images in frequency-time representation: Direction images and resolution map," *Journal of Electronic Imaging,* vol. 19, no. 3 (033012), July-September 2010.

[49] A.M. Grigoryan and Nan Du, "Principle of superposition by direction images," *IEEE Trans. on Image Processing,* vol. 20, no. 9, pp. 2531–2541, September 2011.

[50] A.M. Grigoryan, "Image reconstruction from finite number of projections: Method of transferring geometry," *IEEE Trans. on Image Processing,* vol. 22, no. 12, pp. 4738–4751, December 2013.

[51] A.M. Grigoryan, "Another Step towards Successful Tomographic Imaging in Cancer: Solving the Problem of Image Reconstruction," in book Computer-Aided Cancer Detection and Diagnosis: Recent Advances" (J. Tang and S. Agaian, Editors), *SPIE Press,* chapter 11, pp. 295–338, January 2014.

[52] A.M. Grigoryan, "Comments on "The discrete periodic Radon transform"," *IEEE Trans. on Signal Processing,* vol. 58, no. 11, pp. 5962-5963, Nov 2010.

[53] T. Hsung, D.P.K. Lun, and W. Siu, "Reply to Comments on The Discrete Periodic Radon Transform," *IEEE Trans. on Signal Processing,* vol. 58, no. 11, pp. 5963-5964, Nov 2010.

[54] A.M. Grigoryan, S.S. Agaian, "Alpha-rooting method of color image enhancement by discrete quaternion Fourier transform," [9019-3], in Proc. *SPIE 9019, Image Processing: Algorithms and Systems XII,* 901904 (25 February 2014); 12 p., doi: 10.1117/12.2040596

[55] S.S. Agaian, K. Panetta, A.M. Grigoryan, "A new measure of image enhancement," in Proc. of the IASTED International Conference on Signal Processing & Communication, Marbella, Spain, Sep. 19-22, 2000.

[56] F.T. Arslan, A.M. Grigoryan, "Fast splitting α-rooting method of image enhancement: Tensor representation," *IEEE Trans. on Image Processing,* vol. 15, no. 11, pp. 3375–3384, Nov. 2006.

[57] A.M. Grigoryan, E.R. Dougherty, S.S. Agaian, "Optimal Wiener and Homomorphic Filtration: Review," *Signal Processing,* vol. 121, pp. 111–138, April 2016, (doi:10.1016/j.sigpro.2015.11.006)

[58] A.M. Grigoryan, S.S. Agaian, "Tensor transform-based quaternion Fourier transform algorithm," *Information Sciences*, vol. 320, pp. 62-74, November 2015, (doi: http://dx.doi.org/10.1016/j.ins.2015.05.018)

[59] A.M. Grigoryan and S.S. Agaian, "Cell Phone Camera Color Medical Imaging via Fast Fourier Transform," chapter 3, pp. 33–76, in book Mobile Imaging for Healthcare Applications, (J. Tang, S. Agaian, and J. Tan, Editors), *SPIE Press,* January 2016.

[60] A.M. Grigoryan and S.S. Agaian, "Color Enhancement and Correction for Camera Cell Phone Medical Images Using Quaternion Tools," chapter 4, pp. 77–117, in book Mobile Imaging for Healthcare Applications, (J. Tang, S. Agaian, and J. Tan, Editors), *SPIE Press,* January 2016.

Biography

Artyom M. Grigoryan received the PhD degree in Mathematics and Physics from Yerevan State University (1990). He is an associate Professor of the Department of Electrical Engineering in the College of Engineering, University of Texas at San Antonio. The author of three books, 9 book-chapters, 3 patents and more than 120 papers and specializing in the design of robust filters, fast transforms, tensor and paired transforms, discrete tomography, quaternion imaging, image encryption, processing biomedical images.